Ecosystems
https://doi.org/10.1007/s10021-022-00760-x

Sclerophyllous Forest Tree Growth Under the Influence of a Historic Megadrought in the Mediterranean Ecoregion of Chile

A. Venegas-González,[1,2]* A. A. Muñoz,[3,4,5] S. Carpintero-Gibson,[1] A. González-Reyes,[1] I. Schneider,[3,5] T. Gipolou-Zuñiga,[6] I. Aguilera-Betti,[3,7,8] and F. A. Roig[1,9]

[1]*Hémera Centro de Observación de la Tierra, Escuela de Ingeniería Forestal, Facultad de Ciencias, Universidad Mayor, Camino La Pirámide 5750, Huechuraba, Santiago, Chile;* [2]*Instituto de Ciencias Agroalimentarias, Animales y Ambientales (ICA3), Universidad de O'Higgins, San Fernando, Chile;* [3]*Instituto de Geografía, Pontificia Universidad Católica de Valparaíso, Valparaíso, Chile;* [4]*Centro de Acción Climática, Pontificia Universidad Católica de Valparaíso, Valparaíso, Chile;* [5]*Center for Climate and Resilience Research, Santiago, Chile;* [6]*Laboratorio de Dendrocronología y Cambio Global, Instituto de Conservación, Biodiversidad y Territorio, Facultad de Ciencias Forestales y Recursos Naturales, Universidad Austral de Chile, Valdivia, Chile;* [7]*Programa de Doctorado en Ciencias Antárticas y Subantárticas, Universidad de Magallanes, Punta Arenas, Chile;* [8]*Centro Transdisciplinario de Estudios Ambientales y Desarrollo Humano Sostenible (CEAM), Universidad Austral de Chile, Valdivia, Chile;* [9]*Laboratorio de Dendrocronología e Historia Ambiental, IANIGLA-CONICET-Universidad Nacional de Cuyo, Mendoza, Argentina*

Abstract

The Mediterranean-type Ecosystems of Central Chile is one of the most threatened regions in South America by global change, particularly evidenced by the historical megadrought that has occurred in central Chile since 2010. The sclerophyllous forest stands out, whose history and relationship with drought conditions has been little studied. *Cryptocarya alba* and *Beilschmiedia miersii* (Lauraceae), two large endemic trees, represent an opportunity to analyze the incidence of intense droughts in the growth of sclerophyllous forests by analyzing their tree rings. Here, we considered > 400 trees from nineteen populations of *C. alba* and *B. miersii* growing across a latitudinal gradient (32°–35° S). To study the influence of local and large-scale climatic variability on tree growth, we first grouped the sites by species and explored the relationships between tree-growth patterns of *C. alba* and *B. miersii* with temperature, precipitation, and climate water deficit (CWD). Second, we performed Principal Component Analysis to detect common modes of variability and to explore relationships between growth patterns and their relationship to Palmer Drought Severity Index (PDSI), ENSO and SAM indices. We detected a breaking point as of 2002 at regional level, where a persistent and pronounced decrease in tree growth occurred, mainly influenced by the increase in CWD and the decrease in winter-spring rainfall. In addition, a positive (negative) relationship was showed between PC1 growth-PDSI and PC1 growth-ENSO (growth-SAM), that is, growth increases (decreases) in the same direction as PDSI and ENSO (SAM). Despite the fact that sclero-

Received 24 May 2021; accepted 13 March 2022

Supplementary Information: The online version contains supplementary material available at https://doi.org/10.1007/s10021-022-00760-x.

Author contributions: AVG and AAM conceived the manuscript and idea designed the field sampling; AVG, IS, TGZ and IAB collected the samples and conducted the lab work; AVG, SGC and AGR conducted the statistical analyses and produced figures and tables; AVG led the writing of the manuscript; AVG, AAM and FR contributed critically to the writing. All authors gave final approval for publication.

**Corresponding author; e-mail:* alejandro.venegas@umayor.cl

Published online: 25 May 2022

phyllous populations are highly resistant to drought events, we suggest that the sclerophyllous populations studied here experienced a generalized growth decline, and possibly the natural dynamics of their forests have been altered, mainly due to the accumulating effects of the unprecedented drought since 2010.

Graphical abstract

Key words: *Beilschmiedia miersii*; Chilean forests.; *Cryptocarya alba*; dendroecology.; global change.; increased drought condition.; mediterranean forests.; tree rings.

Highlights

- Tree growth patterns of two sclerophyllous trees species of Chile were studied.
- We detected a growth decline since 2002 at regional level
- This growth decline was increased by sustained drought over the last decade.

Introduction

Climate change has occasioned an increase in the intensity and severity of climate extreme events in many regions (Allen and others 2015). This widespread global phenomenon of warming and drought has caused an impact on forest ecosystem natural dynamics in different biomes, increasing foliar senescence, forest decline, mortality events of tree species, and massive forest diebacks (Allen and others 2010; Greenwood and others 2017). Most of those recent studies have been based on tree-ring analysis (i.e., dendrochronology), which is the main method to study annual sensitivity of tree growth to climate variability at different spatial scales (Schweingruber 1996). Therefore, expanding the dendrochronological network in poorly explored forest types and species is a current challenge for many ecosystems worldwide. Such urgency is further enhanced where climate change interacts with habitat loss in ecosystems with high biodiversity and endemism such occur in the Mediterranean-type Ecosystems of Central Chile (MECC).

Droughts in the Mediterranean basin have intensified toward the end of the twentieth century compared to their natural variability over the last 900 years (Cook and others 2016), which has caused an alteration in the natural growth dynamics of many Mediterranean tree species in Europe and North America (for example, Negron and others 2009; Gea-Izquierdo and Cañellas 2014; Sánchez-Salguero and others 2015; Serra-Maluquer and others 2019). It is predicted that by the year 2100 the Mediterranean regions will experience a change in their biological diversity due to global change (Sala and others 2000; Seager and others 2019). Such predictions and the global relevance of Mediterranean forests demand a better understanding of the alterations of forest dynamics triggered by climate change, particularly in areas of the world that have been little investigated, such as the forests of MECC.

The MECC (30°–38° S) contains the only Mediterranean forests of South America, which are located both at the Coastal and Andes mountains in central Chile (Donoso 1982; Armesto and others 1995). These forests contain a high diversity of endemic plants, so they have been declared a biodiversity hotspot (Arroyo and others 2006). Historically they have been greatly impacted by anthropogenic activities, which has caused a considerable decrease in their natural vegetation cover, mainly due to their substitution by agricultural and forestry crops, urban expansion, overgrazing, unsustainable logging, forest fires and now, due to climate change (Schulz and others 2010; Miranda and others 2016). This biome includes sclerophyllous forests (evergreen trees) in valleys and hillsides, and mountain tree species such as *Nothofagus macrocarpa* and *Austrocedrus chilensis* forests. Matskovsky and others (2021) have shown a generalized forest decline in these forests in recent decades and they have predicted that their growth will be highly threatened in the near future, which can be extended to other tree species in MECC. However, it is still unknown how the sclerophyllous forest

responds to current climate change at lower altitudes (< 1,200 m a.s.l.).

Sclerophyllous tree species in the MECC are characterized by developing xeromorphic and evergreen leaves, which allow them to resist the dry season during spring–summer (from 5 to 7 months according to Donoso 1982). These sclerophyllous forests develops in an intricate topographic matrix of streams and exposures. The forests located on slopes of southern exposure and near rivers present more humid conditions than forests developed on slopes of northern exposure. Therefore, more favorable conditions for growth are found in the first case compared to the second. It is also usual to find older and larger trees on southern slopes, as occurs with the species *Cryptocarya alba* (Molina) Looser (Peumo) and *Beilschmiedia miersii* (Gay) Kosterm (Belloto del Norte). Here, we explored the tree growth response to climate change in a latitudinal gradient across the MECC, using *C. alba* and *B. miersii* as indicator species of the effect of severe droughts in these ecosystems. Since 2010, central Chile has been affected by an uninterrupted sequence of dry years provoking annual rainfall deficits (25–45%) at regional level. Compared to the instrumental historical period during the last century, this hydric phenomenon has been recognized as a megadrought (Garreaud and others 2017, 2020). The global climate models predict for MECC that the observed drying/warming trends will continue by the year 2100 (Bozkurt and others 2018; Fernández and others 2021), a fact that would negatively affect the tree growth of mountain trees (Matskovsky and others 2021). In addition, one-third of the Mediterranean forest have experienced a significant NDVI decrease between 2010 and 2017, indicating the incidence of drought on forest productivity (Miranda and others 2020). Based on these antecedents, we expected that the most populations with *C. alba* and *B. miersii* present a growth decline, with low variability in response to drought among sites. Both tree species belongs to the Lauraceae family, which stands out for having a high dendrochronological potential (Reis-Avila and Oliveira 2017), although they have not been studied in MECC to date. The following objectives have been proposed in this contribution: (i) to develop a new tree-ring network of mesic sclerophyllous forest represented by 19 populations of *C. alba* and *B. miersii*; (ii) to analyze their growth sensitivity to local climate variability; (iii) to analyze the long-term tree-growth trends and their link with recent drought events; and (iv) to explore potential relationships between tree growth and climate variability at regional and large geographic scales.

Materials and Methods

Study Area and Tree Species Populations

We sampled increment cores of 19 sclerophyllous tree populations from 15 sites (Figure 1a, Table 1) along an approximately 400 km of a latitudinal gradient in MECC, and they represented by the species *Cryptocarya alba* and *Beilschmiedia miersii* (Lauraceae family). The annual climate conditions of the studied area varied from 14.1°C to 16.0 °C in mean temperature, from 256 to 792 mm in annual precipitation, and from 154 to 256 mm during the summer months with water deficit (CWD) (Table 1). However, these mean values may varied site-by-site depending on latitude (32.16°–35.53° S) and altitude (100–1150 m a.s.l). From each population, wood samples from 13 to 60 adult trees (DBH > 25 cm, except for TIN and PSJ with DBH > 15 cm) were sampled by non-destructive methods (increment borer), totalizing > 400 trees (Table 1, S1).

Both studied species are endemic, evergreen and dominant in their own communities. *C. alba* conform shrubland communities of MECC, growing in both mountain ranges up to 1500 m.a.s.l. Trees may reach up to 20 m in height and 80–100 m in DBH, with straight or slightly twisted trunk, branched, and with ascending branches (Rodríguez Ríos and others 1983). *B. miersii* is an endemic and dominant tree of relict communities, which can reach 30 m tall and a DBH above 100 cm (Rodríguez Ríos and others 1983).

The region in which our species under study are distributed corresponds to the Mediterranean-type forests of central Chile, both at the Coastal and Andes mountains. Shrubland and thorn steppes cover most of the lower hillslopes and piedmont, which are dominated by open forests of evergreen and sclerophyllous tree species, mainly on southern orientation slopes (0–1200 m.a.s.l). Soils of the Andes mountain are originated from volcanic or granitic rocks and from glacial sediments (Villagrán 1995). Along the Coastal range, soils are formed from granitic rocks and are poorly developed, usually from residuals on rocky outcrops (Donoso 1982; Gajardo 1994). This region is characterized by a typical Mediterranean climate, with rainy and cold winters (June to August), and dry and hot summers (December to March). The total annual precipitation has a year-to-year variation in response to climatic oscillation such as El Niño

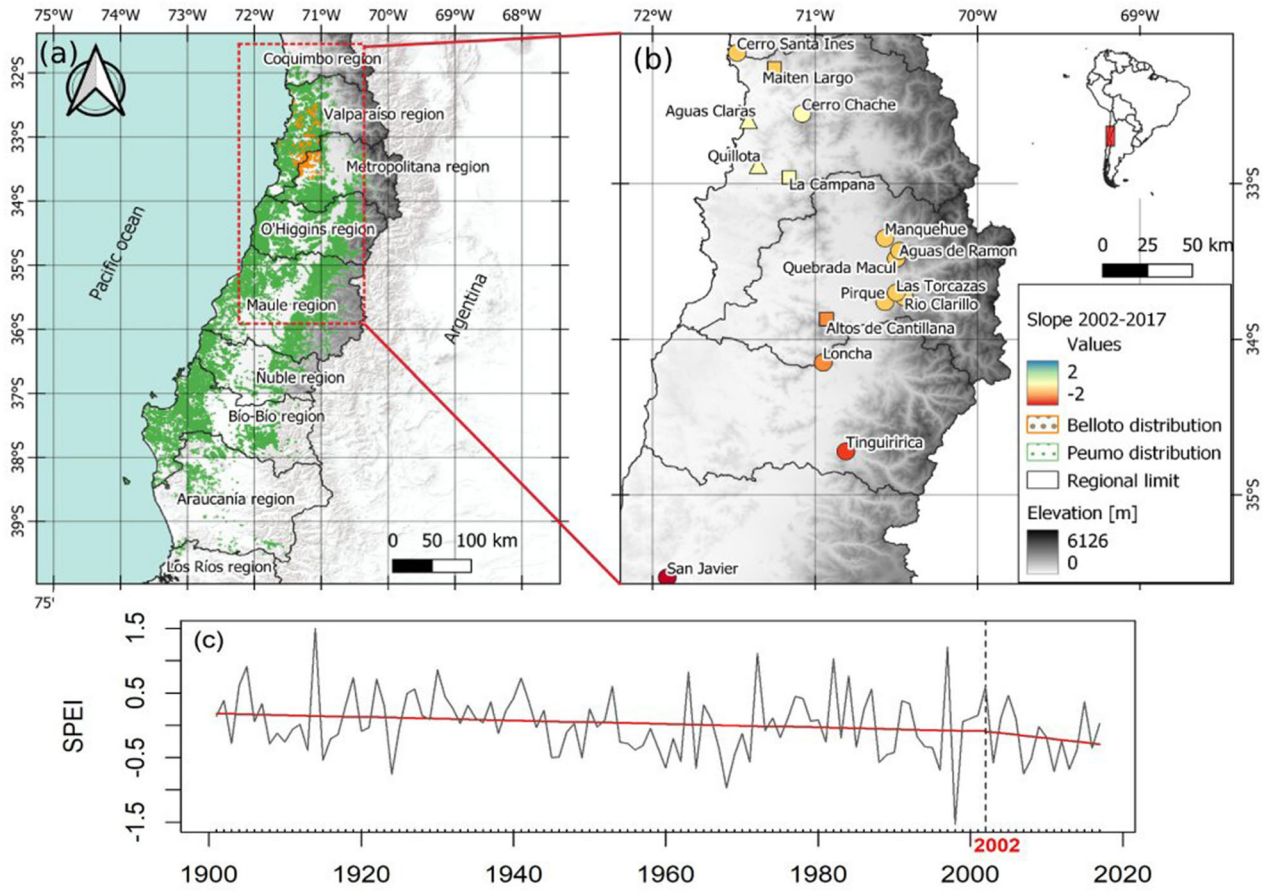

Figure 1. **a** Mediterranean Ecoregion of Chile and location of studied populations. **b** SPEI chronology (May to November) for central Chile (32°–35° S, 70.5°–71.5° W) calculated at one-month scale (dashed blue line) for the period 1901–2017. **c** Slope of SPEI values for period 2002–2017 by sites. Circle, triangle and square represent the populations of *C. alba*, *B. miersii* and both species by site, respectively.

Southern Oscillation (ENSO) and Southern Annular Mode (SAM), that is, more precipitation in El Niño years and less precipitation in positive SAM phase (Garreaud and others 2009).

Tree-Ring Chronologies and Dendroclimatic Analyzes

Each wood sample was processed using the standard dendrochronological methods (Stokes 1996), that is, cores were air dried in the laboratory, glued on wooden supports, sanded with progressively finer sandpaper (80–800 grit) until clearly delineated annual tree-ring boundaries and hence, tree rings were marked under a stereomicroscope for comparison and visual cross-dating with other trees. Ring-width measurements were performed using a Velmex measuring system to a resolution of 0.001 mm. The cross-dating quality was checked with the COFECHA software (Grissino-Mayer 2001), and then, each growth series was standardized to remove the biological age trend or any non-related climatic growth variation by using the ARSTAN software, and hence, we correlated the radial growth with climate variability (Holmes and others 1986). We standardized the individual tree-ring series using either negative exponential, Hugershof or linear fitting detrending functions, depending on the best visual correspondence of fit (Cook and others 1990). We characterized site chronologies using ring widths average and standard error, mean sensitivity (MS), series intercorrelation (SI), Running Bar (RBar), and expressed population signal (EPS) (Fritts 1976). MS represents the mean percentage change of year-to-year growth variability. SI is the mean value of all possible correlations between individual series. RBar describes the mean correlation coefficient for all possible pairings of ring-width series over a common time. AR1 is a measure of the association between tree-ring growths in two consecutive years (Holmes and others 1986). EPS measures the

Table 1. Climatic and Geographical Characteristics (Latitude, Longitude, Altitude) of the Study Sites.

Site	Lat	Lon	Alt. (m.a.s.l)	Pp (mm)	T (°C)	CWD
Cerro Santa Ines[a]	− 32.16	− 71.48	150	269.3	15.0	265.6
Maiten Largo[a,b]	− 32.26	− 71.25	176	256	15.0	272.8
Cerro Chache[a]	− 32.55	− 71.09	643	334.5	16.0	220.3
Aguas Claras[b]	− 32.59	− 71.41	100	279.5	15.3	251.9
Quillota[b]	− 32.88	− 71.35	161	396.6	15.3	245.3
La Campana[a,b]	− 32.96	− 71.16	630	381.0	15.3	243.2
Manquehue[a]	− 33.35	− 70.57	1084	304.5	14.6	187.2
Aguas de Ramón[a]	− 33.43	− 70.48	1152	304.5	14.6	194.5
Quebrada de Macul[a]	− 33.48	− 70.50	1134	505.9	14.4	187.4
Torcazas de Pirque[a]	− 33.71	− 70.48	1126	549.2	14.1	178.5
Rio Clarillo[a]	− 33.73	− 70.45	1000	443.9	14.5	170.2
Pirque[a]	− 33.76	− 70.57	846	443.9	14.5	175.9
Altos de Cantillana[a,b]	− 33.87	− 70.93	414	515.7	14.5	173.1
Loncha[a]	− 34.14	− 70.95	854	481.1	14.8	158.0
Tinguiririca[a]	− 34.72	− 70.81	678	535.7	14.2	181.0
San Javier[a]	− 35.53	− 71.91	140	792.0	14.7	175.7

Values for annual total precipitation, mean total temperature and climatic water deficit are for the period from 1958 to 2017, using gridded climate data of TerraClimate (Abatzoglou and others 2018).
[a]Cryptocarya alba, [b]Beilschmiedia miersii.

strength of the common signal in a chronology over time and verifies the hypothetically perfect chronology, with a theoretical threshold of at least 0.85 (Wigley and others 1984).

To analyze the influence of local climate variability on tree growth, we used monthly precipitation, climatic water deficit CWD, maximum and minimum temperature data from 1958 to 2017 (Abatzoglou and others 2018). The datasets were extracted from the TerraClimate (∼ 4 km spatial resolution) by Google Earth Engine (GEE) Cloud platform. CWD represents the evaporative demand that is not satisfied with available water and, therefore, is an indicator of potential effects of drought stress on trees (Young and others 2017). This index is calculated by the difference between potential evapotranspiration and actual evapotranspiration, and integrates climate, energy loading, drainage, and changes in soil moisture in a single variable. The RESPO.AVG.CLIMATE routine in R free software were implemented to detect robust estimates of the Pearson correlation coefficients in several monthly combinations between ring-width chronologies and climatic data (R core Team 2019; González-Reyes 2020).

Influence of Regional Climate on Tree Growth

We explored the climatic and growth trends at regional level based on piecewise linear models between monthly scale Standardized Precipitation-evapotranspiration Index (SPEI) and tree growth variables (response variables) and the respective calendar years (explanatory variable), using segmented R package (Muggeo 2008). The SPEI is a multiscale drought index that incorporates precipitation and potential evapotranspiration data; negative (positive) values indicate dry (humid) conditions (Vicente-Serrano and others 2010). The data was extracted from the KNMI global climate explorer (https://climexp.knmi.nl/), according to the geographical coordinate of each site (Figure 1), with a spatial resolution of 0.5° from the Climate Research Unit of the University of East Anglia version 4.03. We cut the times series considering a common growth period between 1950 and 2017 and evaluated the change in trends before and after breakpoint from the linear regression coefficient (i.e., slope). The growth variables are ring width and Basal Area Increment (BAI), which depends less on the size of the tree and they are a more representative variable of the growth trends (Camarero and others 2015). Finally, the significance was evaluated using the Kruskall–Wallis test, indicating whether growth increased or decreased after the detected breakpoint (Hollander and Wolfe 1973).

To understand how climatic variables influence the species tree growth after the detected breakpoint by trees species, we modeled the ring widths and BAI (response variable) in function of climatic seasons (autumn, winter, spring and summer)

represented by precipitation (PP), climate water deficit (CWD) and minimum and maximum temperature (T_{min} and T_{max}). We standardized each climate variable on a site-by-site basis by averaging the monthly standard deviations, and we created monthly records of precipitation, CWD, and temperature outputs departures at regional level.

The average seasonal anomalies for the autumn, winter, spring and summer were March–April–May, June–July–August, September–October–November, and December–January–February, respectively. Additionally, for slope model we included categorical variable ''Period'' with two levels, pre- and post-breakpoint. We carried out the logarithmic transformation of growth variables because it presented an asymmetric distribution. In addition, we included as a random factor the trees nested in the sites and the calendar years for growth model, and sites for slope model, with purpose to account for variation in growth due to abiotic characteristics and avoid autocorrelation between series. It should be noted that for growth model annual values were used for the period after breakpoint, while for the second model (slope) regression coefficients before and after breakpoint were used as variables. All models were fitted in R 3.6.1 (R core Team 2019) using the lmer function of the lme4 package following a model building approach (Pinheiro and others 2017). Statistical inference was performed with likelihood ratio tests and the assumptions of the model were verified with classical graphical diagnostics.

Influence of the Global Climate Variability on Tree Growth

To study the influence of large-scale climate variability over tree-growth, we first perform principal component analysis (PCA) to detect common modes of ring-width variability between chronologies. The PCA was runner in R using the psych and GPArotation packages (Bernaards and Jennrich 2005; Revelle 2021). We selected the most relevant patterns spanning 1950–2015. We evaluated relationships via Pearson correlations between detected tree-growth patterns and ENSO and SAM activity. Autoregressive (AR) modeling was used to pre-whitened each time series to remove the effect of first-order autocorrelation AR(1). As an indicator of ENSO, the SST-Niño-3.4 index based on Sea Surface Temperature (SST) variations over the east-central tropical Pacific at 5° N–5° S,170°–120° W was implemented (Trenberth 1997). On the case of SAM, that consists of a barotropic meridional pressure dipole between latitude circles centered at 45° and 60° S and represents the first mode of extra-tropical climate variability in a wide range of time scales in the Southern Hemisphere (Thompson and Wallace 2000; Marshall 2003), we used the SAM-NOAA index. We also explore possible relationships between tree-growth patterns and extratropical regions across the Pacific Ocean, and summarized by the SST Tripole Index (TPI, Henley and others 2015). The TPI is based on the difference between SST's over the central equatorial Pacific and the average of the SST in the Northwest and Southwest Pacific. We used the unfiltered monthly TPI index based on the ERSST V4 data set (Huang and others 2015). Like correlations with local climate, we used the RESPO.AVG.CLIMATE routine in R software (R core Team 2019; González-Reyes 2020).

To understand spatial and temporal drought patterns, independent of our chronologies, we explored relationships between tree-ring growth patterns of *C. alba* and *B. miersii* and the recent South American Drought Atlas SADA (Morales and others 2020). We measured the relationship degree using the Pearson correlation coefficient between our drought patterns and each longitude and latitude grid of SADA, considering the 1950–2000 period. The SADA is based on self-calibrated reconstruction grid by grid integrating tree rings and the Palmer Drought Severity Index PDSI, and is an indicator of dry and wet condition in a specific location or grid. The product presents a spatial resolution of 0.5° × 0.5° longitude and latitude, spanning the 1400–2000 period. All information about SADA, including tree-ring chronologies and PDSI gridded products are freely available in http://www.cr2.cl/datos-dendro-sada/ (CR2 2020).

Results

Characteristics of Tree-Ring Chronologies

We cross-dated 655 ring-width series extracted from 430 trees of *C. alba* and *B. miersii*, covering ages ranging between 32 and 354 years (Table S1). We sampled trees with a mean DBH of 33 cm, being *B. miersii* trees (43.2 ± 3.4 cm) higher than *C. alba* trees (28.8 ± 1.6 cm). The annual growth (average tree-ring width) is similar in both species, with 1.58 ± 1.03 for *C. alba* and 1.77 ± 1.11 for *B. mersii*, being the lowest and highest values found in CSI and PRL (both *C. alba* populations), respectively (Table 2). All sites had high mean sensitivity and intercorrelation values between series (> 0.362 and > 0.488, $p < 0.01$, respectively). RBar varied between 0.192 (CSI) and 0.704 (PML),

Table 2. Characteristics of the Trees Studied From 19 Populations

Site	*Species*	Code	DBH ± SE	RW ± SE	Time span	Age
Cerro Santa Ines	*C. alba*	CSI	23.12 ± 0.89	0.67 ± 0.09	1900–2017	32–258
Maiten Largo	*C. alba*	PML	30.43 ± 1.59	1.94 ± 0.37	1945–2017	44–128
Maiten Largo	*B. miersii*	BML	72.34 ± 4.75	1.80 ± 0.33	1927–2017	60–220
Cerro Chache	*C. alba*	CHA	*	1.02 ± 0.18	1960–2017	42–233
Aguas Claras	*B. miersii*	AGU	*	1.26 ± 0.11	1840–2017	65–348
Quillota	*B. miersii*	QUI	24.47 ± 1.20	2.25 ± 0.24	1968–2017	34–91
Cerro La Campana	*B. miersii*	BLC	31.25 ± 2.19	1.47 ± 0.26	1943–2017	53–105
Cerro La Campana	*C. alba*	PLC	29.89 ± 1.43	1.39 ± 0.26	1933–2017	61–127
Manquehue	*C. alba*	MAN	*	1.93 ± 0.19	1945–2015	45–84
Aguas de Ramón	*C. alba*	ADR	25.86 ± 1.49	1.34 ± 0.20	1869–2017	88–174
Quebrada de Macul	*C. alba*	QDM	16.51 ± 1.33	1.41 ± 0.18	1950–2017	41–97
Torzada de Pirque	*C. alba*	SLT	21.32 ± 1.18	1.42 ± 0.21	1950–2017	41–97
Río Clarillo	*C. alba*	PRC	36.01 ± 1.01	1.92 ± 0.31	1904–2017	48–155
Pirque	*C. alba*	PIR	44.25 ± 2.47	1.53 ± 0.20	1928–2017	52–138
Altos de Cantillana	*B. miersii*	BAC	44.92 ± 5.34	2.06 ± 0.28	1943–2017	53–110
Altos de Cantillana	*C. alba*	PAC	51.71 ± 5.98	2.16 ± 0.39	1928–2017	61–105
Loncha	*C. alba*	PRL	31.46 ± 1.24	2.69 ± 0.33	1930–2017	33–88
Tinguririca	*C. alba*	TIN	15.05 ± 0.38	1.59 ± 0.22	1983–2017	33–77
San Javier	*C. alba*	PSJ	20.03 ± 0.72	1.22 ± 0.15	1950–2017	42–97

Average of diameter at tree diameter at breast height (DBH) and tree-ring width (RW) ± and standard error (SE), minimum and maximum trees age found in the cores, and time span chronology (EPS > 0.85).
**Trees without DBH information.*

and EPS was greater than 0.809 in all populations. AGU and ADR were the populations that provided the longest chronologies of *B. mersii* and *C. alba*, respectively, with an EPS above 0.85 from 1840 to 2017 and from 1869 to 2017, respectively; while those populations with shorter time span for both species were BLC and TIN, with a record period (EPS > 0.85) of 1943–2017 and 1983–2017, respectively (Table S1).

Climate Sensitivity of Tree-Ring Chronologies

Figure 2 show the tree-ring width-climate relationship of 19 populations, which revealed that there is a similar response at the regional level between the different sites along the 400 km of the latitudinal gradient. CWD in autumn–winter (May–August) and early spring (September–October) presents a strong negative correlation in all the sites, except for PLC and PLR that presented a positive relationship during spring (October–December) (Figure 2a). On the contrary, a clear positive influence of precipitation is observed during winter (dormant season) and until late spring-early summer (December–January) of the current growing season for most sites along the latitudinal gradient (Figure 2b). The same negative relationship occurs when comparing CWD with the maximum temperature for the entire growing season, from September to May, and more strongly during spring (Figure 2c). Regarding minimum temperatures, there is a positive relationship during the dormant season (winter), and in some sites this relationship becomes negative during the spring-early summer season (Figure 2d).

Tree-Growth Trends

Although a historical meteorological mega-drought has been recognized since 2010, based on a piecewise linear model between SPEI (response variables) and the respective calendar years (explanatory variable), we have detected that since 2002 there has been a breakpoint in the SPEI series in MECC (Figure 1b). All the studied sites have a negative SPEI trend, showing that the increase in drought conditions since 2002 is observed at the regional level.

In accordance with SPEI trends, we observed a breaking point in the same year in both the ring width and BAI regional tree-ring chronology using both tree species (Figure 3a, b). The regional chronology showed a negative growth trend since 2002, reaching similar values to that observed at the beginning of the second half of the twentieth century (BAI ~ 500 mm^2, Figure 3a, b). The coefficients of the linear regression between the BAI

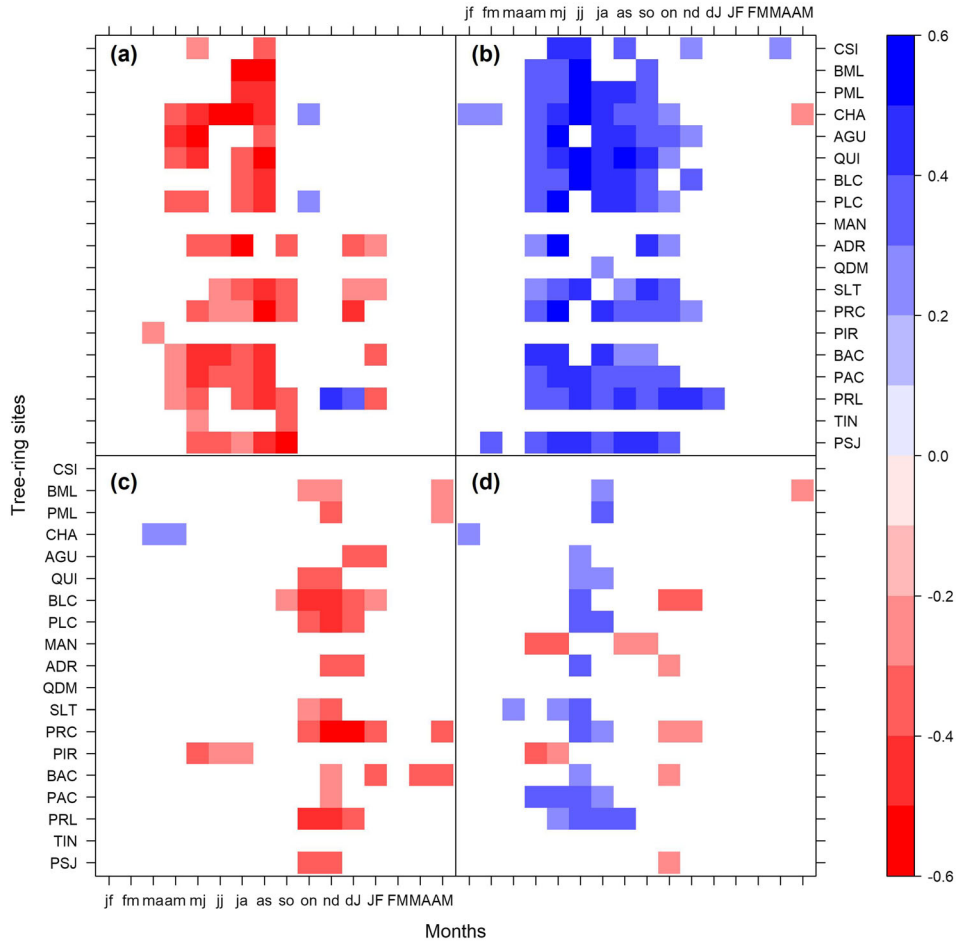

Figure 2. Bimonthly correlation matrix between residual chronologies of 19 studied populations and monthly climatic variables at local scale during 1958–2017. **a** CWD: climatic water deficit, **b** precipitation, **c** maximum temperature, **d** minimum temperature. The current growing season start in September (s) to May (M). Lower case letters indicate calendar year t, while the upper case is $t + 1$. Only significant correlations at the 95% confidence level are shown in color.

and the calendar years before and after the breakpoint, ratify these trends by reversing the sign of the slope, decreasing by up to three times its value and with statistically significant differences (p-value < 0.001; Figure 3c, d). When analyzing site to site, we found that all tree-ring chronologies had negative growth trends for the period 2002–2017 (Figure 2e). However, there are some tree-ring chronologies that did not showed such a drastic change in growth in their trends, such as CSI, CHA and ADR chronologies (Figure 3c). Otherwise, PRL and PML (*C. alba*), and BML (*B. miersii*) presented the lowest slope values, showing that they were one of the most affected sites post-breakpoint (Table S2).

Explanation of Growth Trends by Local Climate

The seasonal climate, mainly during winter and spring, proved to influence growth decline after the 2002 critical point for both species. Most of the total variation for the growth models was explained by random effects, with high values of conditional R^2 (0.64 for *C. alba* and 0.82 for *B. miersii*) and lower values of marginal R^2 (0.06 for *C. alba* and 0.21 for *B. miersii*), being Peumo's model the least valuable. Although the slope model is mainly explained by fixed factors, with at least 31% of variation influenced by climatic parameters (Table 3). The tree-growth reduction for both species is influenced mainly by CWD and precipitation of winter-spring. In this sense, we observed a CWD significative increase and precipitation significative decrease in winter for MECC since 2002 (Figure S3). It should

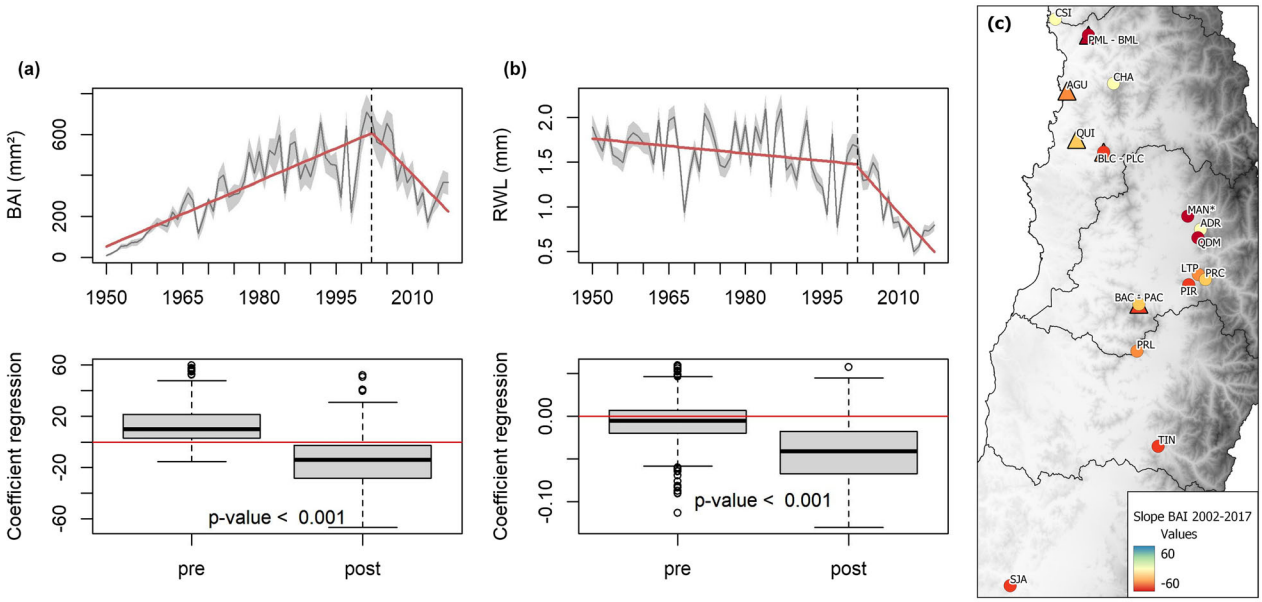

Figure 3. Linear growth trends (red line) and detected breakpoint (segmented line) for all populations for the period 1950–2017, with its 95% confidence interval (gray area). **a** Average basal area increment series (BAI). **b** Ring width series (RWL). The boxplots of coefficients of the linear regressions (slope) between the BAI and RW with the calendar years before (pre) and after (post) the breakpoint detected (2002). **c** Slope of BAI values for period 2002–2017 by tree-ring chronologies. Circle and triangle represent the chronologies of *C. alba* and *B. miersii*, respectively.

be noted that there is a direct relationship between the tree-growth slope and the winter T_{min} in *B. miersii* populations, a variable that trend to decrease during the recent decade.

Climate-Growth Relationship at Regional Scale

The PCA has revealed a high variance concentration retained between the first three principal components (PC1, PC2, and PC3). The PC1 explained the 40.4% of total variance, while PC2 and PC3 have retained the 9% and 7.6%, respectively (Figure S3). Tree-ring sites such as ADR, PRC and BLC have recorded high loadings values on the first principal mode (0.74, 0.76 and 0.65, respectively). To the PC2, the MAN tree-ring site has led the component with a value of 0.94, while the PC3 has led by QDM site (0.97).

Significant relationships were obtained between obtained principal component time-series and large-scale climate forcing from the high latitudes and several regions along the Pacific Ocean, including the tropical region. A positive and significant relationship was recorded between the SST-Niño3.4 index from June to October and the PC1 time series during 1950–2015 ($r = 0.37$; $p < 0.01$; critical $r = \pm 0.31$; Figure 4a). Non-significant relationships were obtained between the PC2, PC3 and SST-Niño 3.4 index as a proxy of ENSO activity. High-latitude climatic forcings as SAM also recorded significant relationships with all PCs time series. The PC1 has registered a significant but negative relationship with the SAM activity of the previous May to previous June ($r = -0.31$; $p < 0.01$; critical $r = \pm 0.31$; Figure 4b). Similar significant results were obtained using the time series after to remove the first order autocorrelation, where Pearson correlation values were equal to -0.3 ($p < 0.05$). A similar negative relationship was obtained between PC2 and SAM of the previous May to the previous June (as the PC1), with a Pearson correlation value of $r = -0.33$ (Figure 4c). The PC3 has recorded a significant and negative relationship with SAM activity from previous October to current October ($r = -0.33$; $p < 0.01$). However, after removing the AR1 into the time series, Pearson correlation values were higher ($r = -0.46$; $p > 0.01$) with respect to the previous obtained value (Figure 4d).

We identified significant relationships between the PC1, PC2 and the SST tripole Index (TPI). Pearson correlation values showed high and positive values between TPI from August to October and the PC1 (Figure 4e; $r = 0.35$, $p < 0.01$) with respect to the PC2 during the previous June to previous July (Figure 4f; $r = 0.27$, $p < 0.05$).

Table 3. Parameter Estimates for the Best Linear Mixed-effect Model (LME) Fitted to Growth Data (log(RWL + 1)) Post-breakpoint and Slope Data (Slope) Pre- and Post- Breakpoint

Variable	Sps	Estimate	Std. error	*t* value	Pr(> Chisq)	R^2m	R^2c
Growth	*Peumo*						
	(Intercept)	5.E-01	8.E-02	5.880	< 0.001	0.059	0.683
	CWD_jja	− 4.E-04	9.E-05	− 4.921	< 0.001		
	PP_jja	3.E-04	8.E-05	4.035	< 0.001		
	CWD_son	8.E-05	3.E-05	2.641	0.008		
	T_{max}_son	9.E-04	6.E-04	1.543	0.123		
	Belloto						
	(Intercept)	− 1.E + 00	4.E-01	− 3.798	< 0.001	0.206	0.824
	CWD_mam	4.E-04	1.E-04	4.493	< 0.001		
	PP_mam	1.E-03	3.E-04	4.058	< 0.001		
	CWD_jja	− 6.E-04	1.E-04	− 5.389	< 0.001		
	CWD_son	− 3.E-04	8.E-05	− 3.689	< 0.001		
	PP_son	4.E-03	8.E-04	4.634	< 0.001		
	T_{max}_dJF	7.E-02	1.E-02	5.501	< 0.001		
Variable	Sps	Estimate	Std. error	*t* value	Pr(> Chisq)	R^2m	R^2c
Slope	*Peumo*						
	(Intercept)	0.002	0.006	0.431	0.666	0.382	0.443
	CWD_mam	− 0.003	0.001	− 3.759	< 0.001		
	CWD_son	0.006	0.001	8.629	< 0.001		
	Periodpost	− 0.097	0.006	− 15.878	< 0.001		
	Belloto						
	(Intercept)	− 0.420	0.062	− 6.768	< 0.001	0.307	0.332
	T_{min}_jja	29.324	4.165	7.041	< 0.001		
	T_{max}_son	19.108	2.895	6.601	< 0.001		
	Periodpost	− 0.713	0.093	− 7.643	< 0.001		

Both, As a function of seasonal climate represented by precipitation (PP), climate water deficit (CWD), maximum temperature (T_{min}) and minimum temperature (T_{min}); and additionally, the categorical variable ''Period'' for the model of the slopes.

Discussion

The analysis of the forest growth responses to global change using different temporal and spatial scales is essential to understand the adaptation capacity of tree species to forecasted climate conditions (Tardif and others 2003; Sánchez-Salguero and others 2017; Matskovsky and others 2021). Here, we present the first record on the dendroclimatic response of two endemic sclerophyllous trees from MECC, *C. alba* and *B. miersii*. Our results showed negative growth trends since the beginning of the twenty-first century (Figure 3), which is explained by climate influence on radial growth (Figure 2, Table 3). We demonstrate that tree-ring chronologies of *C. alba* and *B. miersii* are highly sensitive to local, regional and global climatic variability (Figures 2, 4, 5).

Climatic Signs in Tree Rings

All tree-ring chronologies proved to be sensitive to local climate variability, without a marked biogeographic difference across the latitudinal gradient. Overall, most populations showed a strong dependence of tree growth on winter rains (before the onset of the growing season), that is, they showed a positive (negative) correlation with precipitation (CWD) between May and October, while minimum and maximum temperature had a positive and negative correlation during winter and spring (start of the growing season), respectively. At the species level, it was observed in the *C. alba* populations that the particular conditions of each tree and site would provide larger annual growth variability than the climatic conditions themselves (6% of the variation). However, when we analyzed the model using the growth slopes before and after the breakpoint, we observed that the influence of the local climate increases on tree growth in *C. alba* (38% of the variation). On the other hand, the *B.*

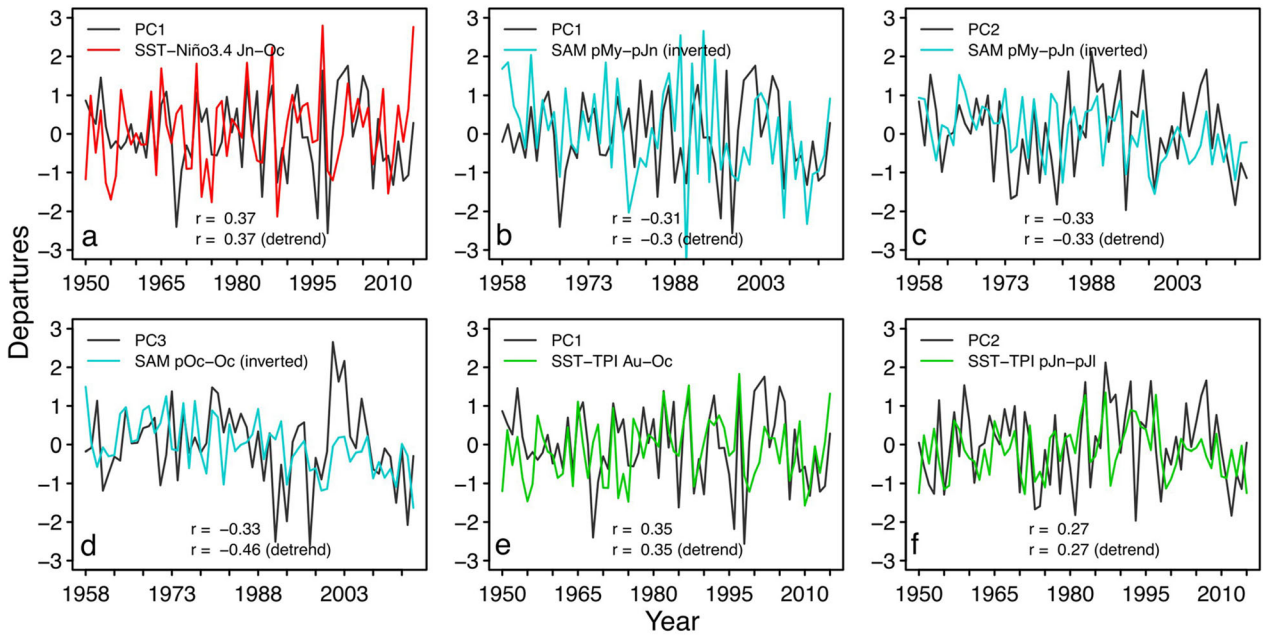

Figure 4. Factor scores of the PC1 time series and **a** SST Niño-3.4, **b** the SAM activity from previous May to previous June. The **c** and **d** panels represent the PC2 and PC3 time series with SAM during previous May to previous June and previous October to October, respectively. All SAM time series have been inverted to the best understanding. The **e** and **f** panels indicate the temporal variations of the PC1 and PC2 factor scores and the SST-Tripole Index TPI during August to October and previous June to previous July, respectively. The detrend *r* Pearson correlations on each panel were calculated removing the AR1 into the time series. SST-Niño 3.4 and SST-TPI were evaluated between 1950 and 2015, while SAM used the 1958–2015 period. The critical *r* Pearson coefficient was significant ($p < 0.05$) when $r = \pm 0.24$ and $r = \pm 0.26$, respectively. The detrend *r* Pearson correlations on each panel were calculated removing the AR1 contained into the time series.

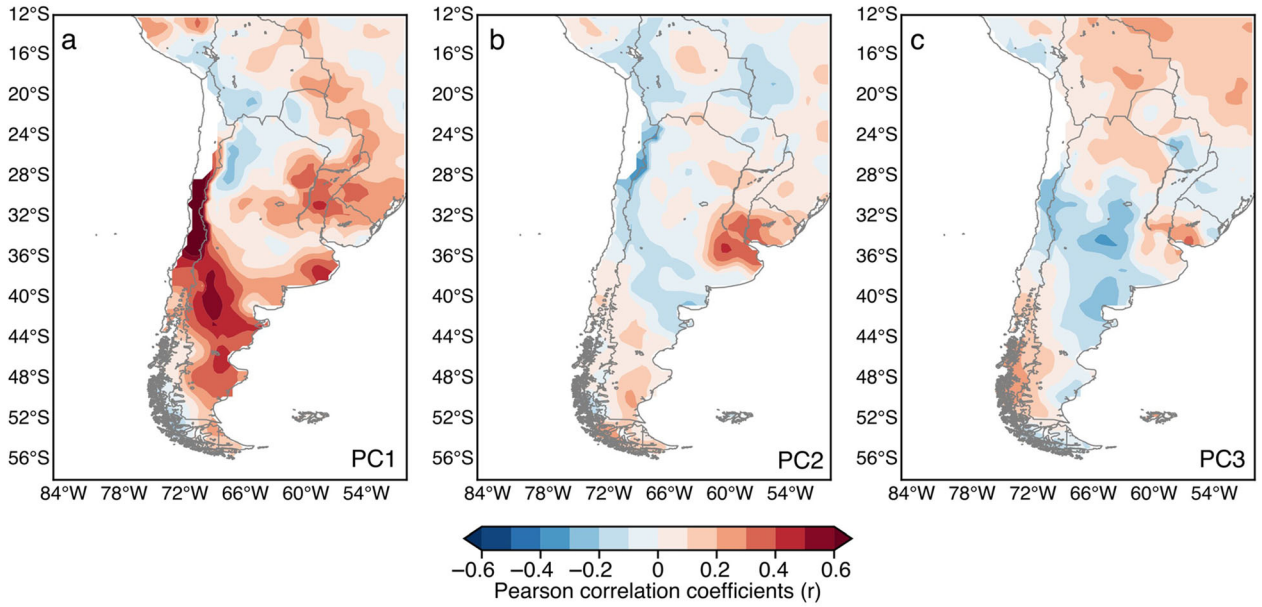

Figure 5. Spatial Pearson correlation coefficients between the **a** PC1, **b** PC2, and **c** the PC3 with the South American Drought Atlas (SADA) based on the scPDSI index (Morales and others 2020). The comparison period was 1950–2000. The critical *r* Pearson coefficient was significant when $r = \pm 0.27$ ($p < 0.05$).

miersii populations are fully influenced by the climate (21 and 31% of the variation in growth and slope models, respectively, Table 3). However, some populations (for example, MAN) showed less sensitivity between climate and growth interrelationships, a fact that is probably explained by microsite factors, since this site is used as an urban park in Santiago de Chile. These results coincide with those observed in other deciduous and native coniferous forests under the Mediterranean climate regime in MECC (Venegas-González and others 2018a, b; Muñoz and others 2020), which suggest a strong effect of droughts in vigor of the vegetation (Garreaud and others 2017).

Spatial and temporal dry and wet patterns inferred by the South American Drought Atlas (SADA) reconstruction exhibited positive relationships with the tree-ring growth patterns, mostly with PC1 during 1950–2000 (Figure 5), which means that tree growth and PDSI variability occurs in phase or in the same direction (increase/decrease growth and PDSI). In a regional context, and using this drought atlas, the regional chronology reveals teleconnections with other South American regions (that is, Patagonia, Altiplano, Argentinian North West region (ANW), and others). These patterns were also shown in the SADA study for Chilean and Argentinean sites (Morales and others 2020), and previously also showed by Muñoz and others (2014) for *Araucaria araucana* growth and soil moisture variations in Argentina, Uruguay and Brazil.

Similar to our results, European Mediterranean forests showed that the increase in the minimum and maximum temperature in summer have a negative influence on radial growth (for example, Gea-Izquierdo and others 2011; Martin-Benito and others 2013; Gea-Izquierdo and Cañellas 2014), both in natural and implanted forests (Sánchez-Salguero and others 2013). Here, we showed the negative influence of the maximum temperatures during spring–summer seasons, which have evidently increased in the last decades at regional level (Figure S2). This is explained by increased evapotranspiration during the growing season (peak growth rates) and soil moisture loss due to evaporation, causing a decrease in primary productivity on both forests and crops in MECC (Bigiarini-Zambrano 2021).

We observed a positive association between tree-ring widths and minimum temperature in winter-early spring in most chronologies. Recently, Matskovsky and others (2021) found that low temperatures during the coldest months becomes the main limiting factor for tree growth in MECC. In other Mediterranean forests, a positive effect of winter-early spring temperature on tree-ring formation has been observed, being the growth limited by low temperatures (for example, Vila and others 2008; Lebourgeois and others 2012; Sánchez-Salguero and others 2015). In the Mediterranean region of Portugal, an increase in the minimum temperature has been observed in winter since 1970, which has favored the tree radial growth (Kurz-Besson and others 2016). However, a significant increase in the minimum temperature has not been observed in winter since 2002, indeed, there is a tendency to decrease the minimum temperature in recent years (Figure S2), which would trigger a decline in tree growth (Figure 3).

The positive relationship that we found between the rainfall of winter-early spring (before the beginning of cambial activity) and ring width, coincides with that it is shown by different authors in Mediterranean forests (for example, Sánchez-Salguero and others 2012; Dorado-Liñán and others 2017). This relationship is confirmed by strong correlations between climate water deficit and radial growth toward the end of the winter-early spring times (Figure 2). This confirms that the main limiting factor in these types of forests is the water availability of the soil, immediately before and during the growing season. Regarding other Mediterranean sclerophyllous species, it has been found that there is a positive correlation between the tree-ring width and the precipitation from autumn to current spring (Campelo and others 2007; Gea-Izquierdo and others 2009; Abrantes and others 2013). In another Chilean Mediterranean mountain tree species, it has been reported that dry years cause a decrease in radial growth, especially during the last decades (Venegas-González and others 2018a). These effect of dry years has been also observed in streamflow reconstructions in the Mediterranean area of Chile, including the Petorca river located in the northern of this geographical range (Muñoz and others 2020), and the Maule river located right in the southern border of this climatic zone (Muñoz and others 2016; Barria and others 2019).

Evidence of Sclerophyllous Forest Decline

The recent increase in temperature and the historical decrease in precipitation experienced in MECC (Boisier and others 2018; Garreaud and others 2020; Matskovsky and others 2021) has affected the tree growth of *C. alba* and *B. miersii* populations, which is evidenced by a significant

breakpoint in growth since 2002. Specifically, the reduction of winter–spring precipitation is the variable that appeared to be most related to forest decline. In other Mediterranean region, many studies have shown a warming-related growth decline in recent decades (Colangelo and others 2017; Gentilesca and others 2017; Navarro-Cerrillo and others 2019; Serra-Maluquer and others 2019; Touhami and others 2019). In the Mediterranean basin, a generalized growth decline of sclerophyllous trees (mainly *Quercus ilex* and *Q. suber*) has been identified since the 1990s, which would be explained by the increase in drought conditions and attacks by different parasitic agents, giving rise to a process of rapid loss of vigor of the trees (Gentilesca and others 2017). Di Filippo and others (2010) showed that tree growth decline of deciduous oaks in Mediterranean environments is linked to a delayed response to climate, mainly caused the water balance during spring-early summer. In Italy, isolated cases of oak decline have been observed since the end of the last century, which has been attributed, in addition to the climate, to the fragmentation of these forests (Gentilesca and others 2017).

Although all chronologies showed a high sensitivity to extreme drought events during the twentieth century (for example, 1968 and 1998, results not shown), it was observed that they continued with a positive growth trend after those years (Figure 3). However, recent changes in climate variability during the last two decades are causing an unprecedented reduction in radial growth. In this sense, it is possible for sclerophyllous species to adapt to unusual extreme droughts. Limousin and others (2009) studied the response of the sclerophyllous species (*Q. ilex*) to rainfall decline, using a rainfall exclusion experiment verifying that this sclerophyllous species, and possibly most of the sclerophyllous species of the Mediterranean biome, have the ability to adapt to future drought conditions through the regulation of stomata, leaf area, and transpiration. Despite these characteristics, we suggest that the sclerophyllous populations studied here experienced a generalized growth decline, and possibly the natural dynamics of their forests have been altered (especially the carbon sequestration and tree regeneration), mainly due to the accumulating effects of the unprecedented drought since 2010. Regeneration absence in *B. miersii* forest in Chile became a challenging topic for forest restoration under climate change (Brito-Rozas and Flores-Toro 2014). Also, recent studies showed drought conditions influence the flammability of *C. alba*, and other exotic trees species from Eucaliptus and Acacia genus (Guerrero and others 2021), creating a new risky factor to be considered to build resilience landscapes in Mediterranean ecoregion of Chile.

Although the historical meteorological megadrought has been recognized since 2010, we have detected that since 2002 there has been a breaking point in the SPEI series in MECC (∼ 32–35° S, 400 km, Figure 1b). Linear climatic trends at the regional level before the breakpoint showed that in all seasons there is a significant increase in the minimum temperature, but not for the maximum temperature (Figure S1). Moreover, we observed that CWD has negative trends in spring and summer, which could indicate that during that time there were no evident long-term drought conditions. However, we observed a significant decrease (increase) in precipitation (CWD) for winter months, while there is a significant increase in maximum and minimum temperature in spring was observed (Figure S2). In addition, we observed that the minimum temperatures that before the breakpoint had significant increases (winter and spring, Figure S1), but lost their significance for the period 2002–2017 (Figure S2). This would be limiting the water consumption by the trees in the season of greatest growth, increasing the soil evaporative rates, and therefore, stressing the plants from the dawn in the morning (the lower temperature hour in MECC). David and others (2007) showed that Mediterranean evergreen trees maintain transpiration rates despite decreasing of the predawn leaf water potential in summer, since more than 70% of the transpired water was being taken from groundwater sources.

In MECC, the groundwater in summer depends to a great extent on precipitation and the level of snow that falls during winter in the Andes Mountains (Taucare and others 2020). However, a decrease in precipitation together with a decline of the snow cover area has been observed in central Chile during the current megadrought, which has possibly caused a considerable decrease in groundwater recharge (Stehr and Aguayo 2017; Duran-Llacer and others 2020; Garreaud and others 2020; Muñoz and others 2020). This situation is even more critical in the Coastal mountain, where the northern studied populations (CSI–PLC) are located, with historical decreases in rainfall, soil moisture, level of lake surfaces, reduction in river flows, and aquifer recharges (Barría and others 2021). Agricultural expansion also competes with native forests for water resources in MECC (Muñoz and others 2020). The ecosystem services of these forest are highly socially and technically accepted,

and they have been proposed in nature based solutions to conservation, restoration and managament of MECC (Schneider and others 2021).

Current Situation of South American Sclerophyllous Trees

Overall, a generalized decline in forest growth promotes conditions of massive tree mortality in the short term (Cailleret and others 2017). Although at the samplings most of the trees were alive, individuals affected by the historic extreme drought of 2019 were noted in several sites (Figure S4). Droughts are stressful for plants due to increases in temperature, vapor pressure deficit, and associated water loss, causing the tree death or indirectly leads to mortality through associated increases in biotic agent infestations (McDowell and others 2020). Hydraulic failure and carbon starvation remain are the physiological processes that explain drought-induced mortality (Adams and others 2017), and both mechanisms are likely to increase the susceptibility of trees to the incidence of insect or disease by pathogens (Gaylord and others 2013). The presence of these opportunistic organisms is a consequence of the loss of vigor of the trees. Outbreak insect herbivores have been reported among the main mortality agents of oak forests, both in Northern America and Europe (Haavik and others 2015), and also in Chilean temperate forest (Estay and others 2019). However, a massive insect attack in the Chilean sclerophyllous forest has not been yet observed, despite extensive browning in *C. alba* populations across MECC (Figure S4). Recently, Miranda and others (2020) showed an unprecedented productivity decline of the sclerophyllous forest in MECC for the period 2000–2017 linked to the megadrought, where the potential resistance loss is suggested by high browning in the driest zones.

However, we still cannot be categorical regarding the incidence of water stress in the sclerophyllous forest, since little is known about its ability to resist future intensification of drought conditions. This hypothesis can be supported because there are historical documents that indicates a massive browning and drying of the Mediterranean forest in 1924, also affecting shrub, mammals, insect populations and domestic cattle (Camus and Jaksic 2020). Only the year 2019 can be consider an extreme drought as the year 1924 was, but the 2019 drought occurred after the driest decade of the last millennium (Garreaud and others 2020; Muñoz and others 2020) and we can expect more impacts on ecosystem services than those caused by the 1924 drought.

Although the influence of age on tree-growth trends was filtered using BAI chronologies (Biondi and Qeadan 2008), we consider that in future studies this approach should be replicated but considering the difference between adult and young trees. Here, we especially studied adult trees, which should have slower growth rates and probably are less sensitive to climate than young trees (Konter and others 2016). However, there is no consensus in the literature on the influence of age on the resilience of Mediterranean forests to drought conditions (Colangelo and others 2017; Granda and others 2018; Serra-Maluquer and others 2018). In MECC, it has been observed that both young, adult or mature trees show a significant decrease in growth since 2000 in mountain trees species (Venegas-González and others 2019), and that the relative resilience to extreme droughts could be explained by tree size and sites influences (Venegas-González and others 2022). However, the influence of DBH/ age on climate sensitivity in sclerophyllous forests is still unknown.

On the other hand, the studies based on stable isotopes have showed a positive trend of water use efficiency, especially in xeric sites, demonstrating the adaptative capacity of Mediterranean species to dry conditions in summer (for example, Maseyk and others 2011; Linares and Camarero 2012; Battipaglia and others 2014; Altieri and others 2015). Based on these findings, we can hypothesize that native trees are stressed, and are probably experiencing an adaptive period, a fact that should be verified by isotopic analyzes or other functional traits. Studies on the resilience of the sclerophyllous forest to climate change are desirable to carry out from the cellular to the landscape scale, expanding the analysis of the impact that droughts can produce on the ecosystem services provided by the MECC forests. Finally, our results constitute an input to detect refuge areas and identify the response capacity of Mediterranean forests to global change.

ACKNOWLEDGEMENTS

We thank for the authorization of the fieldwork and support in the logistics to the Chilean National Forest Corporation (CONAF), and private parks: ''Altos de Cantillana'', ''Cerro Santa Inés'', ''Aguas de Ramón'', ''Bosques de Tinguiririca'', ''Aguas Claras'', among others. AVG was funded by the Rufford Small Grants 25822-2, ANID/FONDECYT 11180992 and ClimatAmsud CLI2020009; and

AAM was supported by ANID/FONDAP/15110009, ANID/FONDECYT 1201714, ESR UCV2095, and PUCV DI 39.431/2020; AGR thanks ANID/PAI/77190101. IAB also thanks to ANID-Subdirección de Capital Humano/Doctorado Nacional/2021-21212335 for the PhD scholarship.

REFERENCES

Abatzoglou JT, Dobrowski SZ, Parks SA, Hegewisch KC. 2018. TerraClimate, a high-resolution global dataset of monthly climate and climatic water balance from 1958–2015. Sci Data 5:1–12.

Abrantes J, Campelo F, Garcia-Gonzalez I, Nabais C. 2013. Environmental control of vessel traits in Quercus ilex under Mediterranean climate: relating xylem anatomy to function. Trees-Structure Funct 27:655–662.

Adams HD, Zeppel MJB, Anderegg WRL, Hartmann H, Landhäusser SM, Tissue DT, Huxman TE, Hudson PJ, Franz TE, Allen CD. 2017. A multi-species synthesis of physiological mechanisms in drought-induced tree mortality. Nat Ecol Evol 1:1285–1291.

Allen CD, Breshears DD, McDowell NG. 2015. On underestimation of global vulnerability to tree mortality and forest die-off from hotter drought in the Anthropocene. Ecosphere 6:1–55.

Allen CD, Macalady AK, Chenchouni H, Bachelet D, McDowell N, Vennetier M, Kitzberger T, Rigling A, Breshears DD, Hogg EHT. 2010. A global overview of drought and heat-induced tree mortality reveals emerging climate change risks for forests. For Ecol Manage 259:660–684.

Altieri S, Mereu S, Cherubini P, Castaldi S, Sirignano C, Lubritto C, Battipaglia G. 2015. Tree-ring carbon and oxygen isotopes indicate different water use strategies in three Mediterranean shrubs at Capo Caccia (Sardinia, Italy). Trees 29:1593–1603.

Armesto J, Villagrán C, Arroyo MK. 1995. Ecología de los bosques nativos. Editor Univ Santiago Chile.

Arroyo MTK, Marquet PA, Marticorena C, Cavieres LA, Squeo FA, Simonetti Zambelli JA, Rozzi R, Massardo F. 2006. El hotspot chileno, prioridad mundial para la conservación. Diversidad de ecosistemas, ecosistemas terrestres.

Barría P, Chadwick C, Ocampo-Melgar A, Galleguillos M, Garreaud R, Díaz-Vasconcellos R, Poblete D, Rubio-Álvarez E, Poblete-Caballero D. 2021. Water management or megadrought: what caused the Chilean Aculeo Lake drying? Reg Environ Chang 21:1–15.

Barria P, Rojas M, Moraga P, Muñoz A, Bozkurt D, Alvarez-Garreton C. 2019. Anthropocene and streamflow: Long-term perspective of streamflow variability and water rights. Elem Sci Anth 7.

Battipaglia G, De Micco V, Brand WA, Saurer M, Aronne G, Linke P, Cherubini P. 2014. Drought impact on water use efficiency and intra-annual density fluctuations in Erica arborea on Elba (Italy). Plant Cell Environ 37:382–391.

Bernaards CA, Jennrich RI. 2005. Gradient Projection Algorithms and Software for Arbitrary Rotation Criteria in Factor Analysis. Educ Psychol Meas 65:676–696. https://doi.org/10.1177/0013164404272507.

Bigiarini-Zambrano F. 2021. Four decades of satellite data for agricultural drought monitoring throughout the growing season in Central Chile.

Biondi F, Qeadan F. 2008. A theory-driven approach to tree-ring standardization: defining the biological trend from expected basal area increment. Tree-Ring Res 64:81–96.

Boisier JP, Alvarez-Garretón C, Cordero RR, Damiani A, Gallardo L, Garreaud RD, Lambert F, Ramallo C, Rojas M, Rondanelli R. 2018. Anthropogenic drying in central-southern Chile evidenced by long-term observations and climate model simulations. Elem Sci Anth 6.

Bozkurt D, Rojas M, Boisier JP, Valdivieso J. 2018. Projected hydroclimate changes over Andean basins in central Chile from downscaled CMIP5 models under the low and high emission scenarios. Clim Change 150:131–147.

Brito-Rozas E, Flores-Toro L. 2014. Structure and dynamics in North Belloto forests (*Beilschmiedia miersii*) in Cordillera El Melón, Valparaíso Region, Chile. Bosque 35:13–21.

Cailleret M, Jansen S, Robert EMR, Desoto L, Aakala T, Antos JA, Beikircher B, Bigler C, Bugmann H, Caccianiga M. 2017. A synthesis of radial growth patterns preceding tree mortality. Glob Chang Biol 23:1675–1690.

Camarero JJ, Gazol A, Sangüesa-Barreda G, Oliva J, Vicente-Serrano SM. 2015. To die or not to die: early warnings of tree dieback in response to a severe drought. J Ecol 103:44–57.

Campelo F, Nabais C, Freitas H, Gutierrez E. 2007. Climatic significance of tree-ring width and intra-annual density fluctuations in Pinus pinea from a dry Mediterranean area in Portugal. Ann for Sci 64:229–238.

Camus P, Jaksic F. 2020. La extraordinaria sequía de 1924: Crisis socio-ecológica e irrupción del poder militar en Chile. Rev Geogr Norte Gd:397–416.

Colangelo M, Camarero JJ, Battipaglia G, Borghetti M, De Micco V, Gentilesca T, Ripullone F. 2017. A multi-proxy assessment of dieback causes in a Mediterranean oak species. Tree Physiol 37:617–631.

Cook BI, Anchukaitis KJ, Touchan R, Meko DM, Cook ER. 2016. Spatiotemporal drought variability in the Mediterranean over the last 900 years. J Geophys Res Atmos 121:2060–2074.

Cook ER, Briffa K, Shiyatov S, Mazepa V. 1990. Tree-ring standardization and growth-trend estimation. Methods dendrochronology Appl Environ Sci:104–23.

CR2. 2020. Atlas Sudamericano de Sequías South American Drought Atlas (SADA) Período 1400–2000 AD. Cent Clim Resil Res. https://www.cr2.cl/datos-dendro-sada/

David TS, Henriques MO, Kurz-Besson C, Nunes J, Valente F, Vaz M, Pereira JS, Siegwolf R, Chaves MM, Gazarini LC. 2007. Water-use strategies in two co-occurring Mediterranean evergreen oaks: surviving the summer drought. Tree Physiol 27:793–803.

Donoso C. 1982. Reseña ecológica de los bosques mediterráneos de Chile. Bosque 4:117–146.

Dorado-Liñán I, Zorita E, Martínez-Sancho E, Gea-Izquierdo G, Di Filippo A, Gutiérrez E, Levanic T, Piovesan G, Vacchiano G, Zang C. 2017. Large-scale atmospheric circulation enhances the Mediterranean East-West tree growth contrast at rear-edge deciduous forests. Agric for Meteorol 239:86–95.

Duran-Llacer I, Munizaga J, Arumí JL, Ruybal C, Aguayo M, Sáez-Carrillo K, Arriagada L, Rojas O. 2020. Lessons to Be Learned: Groundwater Depletion in Chile's Ligua and Petorca Watersheds through an Interdisciplinary Approach. Water 12:2446.

Estay SA, Chávez RO, Rocco R, Gutiérrez AG. 2019. Quantifying massive outbreaks of the defoliator moth Ormiscodes amphimone in deciduous Nothofagus-dominated southern forests

using remote sensing time series analysis. J Appl Entomol 143:787–796.

Fernández A, Schumacher V, Ciocca I, Rifo A, Muñoz AA, Justino F. 2021. Validation of a 9-km WRF dynamical downscaling of temperature and precipitation for the period 1980–2005 over Central South Chile. Theor Appl Climatol 143:361–378.

Di Filippo A, Alessandrini A, Biondi F, Blasi S, Portoghesi L, Piovesan G. 2010. Climate change and oak growth decline: Dendroecology and stand productivity of a Turkey oak (Quercus cerris L.) old stored coppice in Central Italy. Ann for Sci 67:706.

Fritts HC. 1976. Characteristics of tree rings as predictors of climate. Abstr Pap Am Chem Soc 172:30.

Gajardo R. 1994. La vegetación natural de Chile. Clasif y Distrib geográfica Editor Univ Santiago, Chile 33.

Garreaud R, Alvarez-Garreton C, Barichivich J, Boisier JP, Christie D, Galleguillos M, LeQuesne C, McPhee J, Zambrano M. 2017. The 2010–2015 mega drought in Central Chile: Impacts on regional hydroclimate and vegetation. Hydrol Earth Syst Sci:in review.

Garreaud RD, Boisier JP, Rondanelli R, Montecinos A, Sepúlveda HH, Veloso-Aguila D. 2020. The central Chile mega drought (2010–2018): a climate dynamics perspective. Int J Climatol 40:421–439.

Garreaud RD, Vuille M, Compagnucci R, Marengo J. 2009. Present-day South American climate. Palaeogeogr Palaeoclimatol Palaeoecol 281:180–195.

Gaylord ML, Kolb TE, Pockman WT, Plaut JA, Yepez EA, Macalady AK, Pangle RE, McDowell NG. 2013. Drought predisposes piñon–juniper woodlands to insect attacks and mortality. New Phytol 198:567–578.

Gea-Izquierdo G, Cañellas I. 2014. Local climate forces instability in long-term productivity of a Mediterranean oak along climatic gradients. Ecosystems 17:228–241.

Gea-Izquierdo G, Cherubini P, Cañellas I. 2011. Tree-rings reflect the impact of climate change on Quercus ilex L. along a temperature gradient in Spain over the last 100 years. For Ecol Manage 262:1807–1816.

Gea-Izquierdo G, Martín-Benito D, Cherubini P, Isabel C. 2009. Climate-growth variability in Quercus ilex L. west Iberian open woodlands of different stand density. Ann for Sci 66:802.

Gentilesca T, Camarero JJ, Colangelo M, Nole A, Ripullone F. 2017. Drought-induced oak decline in the western Mediterranean region: an overview on current evidences, mechanisms and management options to improve forest resilience. iForest-Biogeosciences for 10:796.

González-Reyes A. 2020. KLIMA_trees. GitHub. https://github.com/lonkotrewa/KLIMA_trees

Granda E, Gazol A, Camarero JJ. 2018. Functional diversity differently shapes growth resilience to drought for co-existing pine species. J Veg Sci 29:265–275.

Greenwood S, Ruiz-Benito P, Martínez-Vilalta J, Lloret F, Kitzberger T, Allen CD, Fensham R, Laughlin DC, Kattge J, Bönisch G. 2017. Tree mortality across biomes is promoted by drought intensity, lower wood density and higher specific leaf area. Ecol Lett 20:539–553.

Grissino-Mayer HD. 2001. Evaluating Crossdating Accuracy: A Manual and Tutorial for the Computer Program COFECHA. Tree-Ring Res 57:205–221.

Guerrero F, Hernández C, Toledo M, Espinoza L, Carrasco Y, Arriagada A, Muñoz A, Taborga L, Bergmann J, Carmona C. 2021. Leaf Thermal and Chemical Properties as Natural Drivers of Plant Flammability of Native and Exotic Tree Species of the Valparaíso Region, Chile. Int J Environ Res Public Health 18:7191.

Haavik LJ, Billings SA, Guldin JM, Stephen FM. 2015. Emergent insects, pathogens and drought shape changing patterns in oak decline in North America and Europe. For Ecol Manage 354:190–205.

Henley BJ, Gergis J, Karoly DJ, Power S, Kennedy J, Folland CK. 2015. A tripole index for the interdecadal Pacific oscillation. Clim Dyn 45:3077–3090.

Hollander M, Wolfe DA. 1973. Kruskal-Wallis: a distribution-free test. In: Nonparametric Statistical Methods. pp 114–37.

Holmes RL, Adams RK, Fritts HC. 1986. Tree-ring chronologies of western North America: California, eastern Oregon and northern Great Basin with procedures used in the chronology development work including users manuals for computer programs COFECHA and ARSTAN.

Huang B, Banzon VF, Freeman E, Lawrimore J, Liu W, Peterson TC, Smith TM, Thorne PW, Woodruff SD, Zhang H-M. 2015. Extended reconstructed sea surface temperature version 4 (ERSST. v4). Part I: Upgrades and intercomparisons. J Clim 28:911–930.

Konter O, Büntgen U, Carrer M, Timonen M, Esper J. 2016. Climate signal age effects in boreal tree-rings: Lessons to be learned for paleoclimatic reconstructions. Quat Sci Rev 142:164–172.

Kurz-Besson CB, Lousada JL, Gaspar MJ, Correia IE, David TS, Soares PMM, Cardoso RM, Russo A, Varino F, Mériaux C. 2016. Effects of recent minimum temperature and water deficit increases on Pinus pinaster radial growth and wood density in southern Portugal. Front Plant Sci 7:1170.

Larsson L. 2014. CooRecorder and Cdendro programs of the CooRecorder/Cdendro package version 7.7.

Lebourgeois F, Mérian P, Courdier F, Ladier J, Dreyfus P. 2012. Instability of climate signal in tree-ring width in Mediterranean mountains: a multi-species analysis. Trees 26:715–729.

Limousin JM, Rambal S, Ourcival JM, Rocheteau A, Joffre R, Rodriguez-Cortina R. 2009. Long-term transpiration change with rainfall decline in a Mediterranean Quercus ilex forest. Glob Chang Biol 15:2163–2175.

Linares JC, Camarero JJ. 2012. From pattern to process: linking intrinsic water-use efficiency to drought-induced forest decline. Glob Chang Biol 18:1000–1015.

Marshall GJ. 2003. Trends in the southern annular mode from observations and reanalyses. J Clim 16:4134–4143.

Martin-Benito D, Beeckman H, Canellas I. 2013. Influence of drought on tree rings and tracheid features of Pinus nigra and Pinus sylvestris in a mesic Mediterranean forest. Eur J for Res 132:33–45.

Maseyk K, Hemming D, Angert A, Leavitt SW, Yakir D. 2011. Increase in water-use efficiency and underlying processes in pine forests across a precipitation gradient in the dry Mediterranean region over the past 30 years. Oecologia 167:573–585.

Matskovsky V, Venegas-González A, Garreaud R, Roig FA, Gutiérrez AG, Muñoz AA, Le Quesne C, Klock K, Canales C. 2021. Tree growth decline as a response to projected climate change in the 21st century in Mediterranean mountain forests of Chile. Glob Planet Change 198:103406.

McDowell NG, Allen CD, Anderson-Teixeira K, Aukema BH, Bond-Lamberty B, Chini L, Clark JS, Dietze M, Grossiord C,

Hanbury-Brown A, Hurtt GC, Jackson RB, Johnson DJ, Kueppers L, Lichstein JW, Ogle K, Poulter B, Pugh TAM, Seidl R, Turner MG, Uriarte M, Walker AP, Xu C. 2020. Pervasive shifts in forest dynamics in a changing world. Science (80-) 368.

Miranda A, Altamirano A, Cayuela L, Lara A, González M. 2016. Native forest loss in the Chilean biodiversity hotspot: revealing the evidence. Reg Environ Chang:1–13.

Miranda A, Lara A, Altamirano A, Di Bella C, González ME, Camarero JJ. 2020. Forest browning trends in response to drought in a highly threatened mediterranean landscape of South America. Ecol Indic 115:106401.

Morales MS, Cook ER, Barichivich J, Christie DA, Villalba R, LeQuesne C, Srur AM, Ferrero ME, González-Reyes Á, Couvreux F. 2020. Six hundred years of South American tree rings reveal an increase in severe hydroclimatic events since mid-20th century. Proc Natl Acad Sci 117:16816–16823.

Muggeo VMR. 2008. Segmented: an R package to fit regression models with broken-line relationships. R News 8:20–25.

Muñoz AA, Barichivich J, Christie DA, Dorigo W, Sauchyn D, González-Reyes Á, Villalba R, Lara A, Riquelme N, González ME. 2014. Patterns and drivers of A raucaria araucana forest growth along a biophysical gradient in the northern P atagonian A ndes: Linking tree rings with satellite observations of soil moisture. Austral Ecol 39:158–169.

Muñoz AA, González-Reyes A, Lara A, Sauchyn D, Christie D, Puchi P, Urrutia-Jalabert R, Toledo-Guerrero I, Aguilera-Betti I, Mundo I. 2016. Streamflow variability in the Chilean Temperate-Mediterranean climate transition (35° S–42° S) during the last 400 years inferred from tree-ring records. Clim Dyn:1–16.

Muñoz AA, Klock-Barría K, Alvarez-Garreton C, Aguilera-Betti I, González-Reyes Á, Lastra JA, Chávez RO, Barría P, Christie D, Rojas-Badilla M. 2020. Water crisis in Petorca Basin, Chile: The combined effects of a mega-drought and water management. Water 12:648.

Navarro-Cerrillo RM, Sarmoum M, Gazol A, Abdoun F, Camarero JJ. 2019. The decline of Algerian Cedrus atlantica forests is driven by a climate shift towards drier conditions. Dendrochronologia 55:60–70.

Negron JF, McMillin JD, Anhold JA, Coulson D. 2009. Bark beetle-caused mortality in a drought-affected ponderosa pine landscape in Arizona, USA. For Ecol Manage 257:1353–1362.

Pinheiro J, Bates D, DebRoy S, Sarkar D. 2017. nlme: linear and nonlinear mixed effects models.

R core Team. 2019. R: A Language and Environment for Statistical Computing. R Found Stat Comput. https://www.r-project.org/

Reis-Avila G, Oliveira JM. 2017. Lauraceae: A promising family for the advance of neotropical dendrochronology. Dendrochronologia 44:103–116.

Revelle W. 2021. psych: Procedures for Psychological, Psychometric, and Personality Research. Northwest Univ. https://cran.r-project.org/package=psych

Rodríguez Ríos R, Matthei S, Quezada M. 1983. Flora arbórea de Chile.

Sala OE, Chapin FS, Armesto JJ, Berlow E, Bloomfield J, Dirzo R, Huber-Sanwald E, Huenneke LF, Jackson RB, Kinzig A. 2000. Global biodiversity scenarios for the year 2100. Science (80-) 287:1770–1774.

Sánchez-Salguero R, Camarero JJ, Carrer M, Gutiérrez E, Alla AQ, Andreu-Hayles L, Hevia A, Koutavas A, Martínez-Sancho E, Nola P. 2017. Climate extremes and predicted warming threaten Mediterranean Holocene firs forests refugia. Proc Natl Acad Sci 114:E10142–E10150.

Sánchez-Salguero R, Camarero JJ, Dobbertin M, Fernández-Cancio Á, Vilà-Cabrera A, Manzanedo RD, Zavala MA, Navarro-Cerrillo RM. 2013. Contrasting vulnerability and resilience to drought-induced decline of densely planted vs. natural rear-edge Pinus nigra forests. For Ecol Manage 310:956–967.

Sánchez-Salguero R, Camarero JJ, Hevia A, Madrigal-González J, Linares JC, Ballesteros-Canovas JA, Sánchez-Miranda A, Alfaro-Sánchez R, Sangüesa-Barreda G, Galván JD. 2015. What drives growth of Scots pine in continental Mediterranean climates: drought, low temperatures or both? Agric for Meteorol 206:151–162.

Sánchez-Salguero R, Navarro-Cerrillo RM, Camarero JJ, Fernández-Cancio Á. 2012. Selective drought-induced decline of pine species in southeastern Spain. Clim Change 113:767–785.

Schneider I, Brito-Escudero C, Aguilera-Betti I, Klock-Barría K, Saldes-Cortés A, Celis-Diez J, Ugalde A, Jorquera-Martínez L, Venegas-Gonzalez A, Carvallo G, Muñoz A. 2021. Soluciones de base Natural (SbN) para conflictos de escasez hídrica en la Ecorregión Mediterránea de Chile. Rev Geogr Norte Gd.

Schulz JJ, Cayuela L, Echeverria C, Salas J, Benayas JMR. 2010. Monitoring land cover change of the dryland forest landscape of Central Chile (1975–2008). Appl Geogr 30:436–447.

Schweingruber FH. 1996. Tree rings and environment: dendroecology. Paul Haupt AG Bern

Seager R, Osborn TJ, Kushnir Y, Simpson IR, Nakamura J, Liu H. 2019. Climate variability and change of Mediterranean-type climates. J Clim 32:2887–2915.

Serra-Maluquer X, Gazol A, Sangüesa-Barreda G, Sánchez-Salguero R, Rozas V, Colangelo M, Gutiérrez E, Camarero JJ. 2019. Geographically Structured Growth decline of Rear-Edge Iberian Fagus sylvatica Forests After the 1980s Shift Toward a Warmer Climate. Ecosystems 22:1325–1337.

Serra-Maluquer X, Mencuccini M, Martínez-Vilalta J. 2018. Changes in tree resistance, recovery and resilience across three successive extreme droughts in the northeast Iberian Peninsula. Oecologia 187:343–354.

Stehr A, Aguayo M. 2017. Snow cover dynamics in Andean watersheds of Chile (32.0–39.5 S) during the years 2000–2016. Hydrol Earth Syst Sci 21:5111–5126.

Stokes MA. 1996. An introduction to tree-ring dating. University of Arizona Press.

Tardif J, Camarero JJ, Ribas M, Gutiérrez E. 2003. Spatiotemporal variability in tree growth in the Central Pyrenees: climatic and site influences. Ecol Monogr 73:241–257.

Taucare M, Daniele L, Viguier B, Vallejos A, Arancibia G. 2020. Groundwater resources and recharge processes in the Western Andean Front of Central Chile. Sci Total Environ 722:137824.

Thompson DWJ, Wallace JM. 2000. Annular modes in the extratropical circulation. Part I: Month-to-Month Variability. J Clim 13:1000–1016.

Touhami I, Chirino E, Aouinti H, El Khorchani A, Elaieb MT, Khaldi A, Nasr Z. 2019. Decline and dieback of cork oak (Quercus suber L.) forests in the Mediterranean basin: A case study of Kroumirie, Northwest Tunisia. J For Res:1–17.

Trenberth KE. 1997. The definition of El Nino. Bull Am Meteorol Soc 78:2771–2777.

Venegas-González A, Gibson-Capintero S, Anholetto-Junior C, Mathiasen P, Premoli AC, Fresia P. 2022. Tree-ring analysis and genetic associations help to understand drought sensitivity in the Chilean Endemic Forest of Nothofagus macrocarpa. Front For Glob Change 5:762347.

Venegas-González A, Roig F, Gutiérrez AG, Peña-Rojas K, Tomazello Filho M. 2018a. Efecto de la variabilidad climática sobre los patrones de crecimiento y establecimiento de *Nothofagus macrocarpa* en Chile central. Bosque (valdivia) 39:81–93.

Venegas-González A, Roig FA, Gutiérrez AG, Tomazello Filho M. 2018b. Recent radial growth decline in response to increased drought conditions in the northernmost *Nothofagus* populations from South America. For Ecol Manage 409:94–104.

Venegas-González A, Roig FA, Peña-Rojas K, Hadad MA, Aguilera-Betti I, Muñoz AA. 2019. Recent consequences of climate change have affected tree growth in distinct *Nothofagus macrocarpa* (DC.) FM Vaz & Rodr age classes in Central Chile. Forests 10.

Vicente-Serrano SM, Beguería y S, López-Moreno JI. 2010. A multiscalar drought index sensitive to global warming: the standardized precipitation evapotranspiration index. Journal of Climate 23(7):1696–1718.

Vila B, Vennetier M, Ripert C, Chandioux O, Liang E, Guibal F, Torre F. 2008. Has global change induced opposite trends in radial growth of Pinus sylvestris and Pinus halepensis at their bioclimatic limit? The example of the Sainte-Baume forest (south-east France). Ann For Sci:9.

Villagrán CM. 1995. Quaternary history of the Mediterranean vegetation of Chile. Ecology and biogeography of Mediterranean ecosystems in Chile. Springer: California, and Australia. pp 3–20.

Wigley TML, Briffa KR, Jones PD. 1984. On the average value of correlated time-series, with applications in dendroclimatology and hydrometeorology. J Clim Appl Meteorol 23:201–213.

Young DJN, Stevens JT, Earles JM, Moore J, Ellis A, Jirka AL, Latimer AM. 2017. Long-term climate and competition explain forest mortality patterns under extreme drought. Ecol Lett 20:78–86.